

Dynamic Assessment of COTS Converters-based DC Integrated Power Systems in Electric Ships

Francés, Airán ; Anvari-Moghaddam, Amjad; Diaz, Enrique Rodriguez; Quintero, Juan Carlos Vasquez; Guerrero, Josep M.; Uceda, Javier

Published in:
I E E E Transactions on Industrial Informatics

DOI (link to publication from Publisher):
[10.1109/TII.2018.2810323](https://doi.org/10.1109/TII.2018.2810323)

Publication date:
2018

Document Version
Accepted author manuscript, peer reviewed version

[Link to publication from Aalborg University](#)

Citation for published version (APA):
Francés, A., Anvari-Moghaddam, A., Diaz, E. R., Quintero, J. C. V., Guerrero, J. M., & Uceda, J. (2018). Dynamic Assessment of COTS Converters-based DC Integrated Power Systems in Electric Ships. *I E E E Transactions on Industrial Informatics*, 14(12), 5518-5529. <https://doi.org/10.1109/TII.2018.2810323>

General rights

Copyright and moral rights for the publications made accessible in the public portal are retained by the authors and/or other copyright owners and it is a condition of accessing publications that users recognise and abide by the legal requirements associated with these rights.

- Users may download and print one copy of any publication from the public portal for the purpose of private study or research.
- You may not further distribute the material or use it for any profit-making activity or commercial gain
- You may freely distribute the URL identifying the publication in the public portal -

Take down policy

If you believe that this document breaches copyright please contact us at vbn@aub.aau.dk providing details, and we will remove access to the work immediately and investigate your claim.

Dynamic Assessment of COTS Converters-based DC Integrated Power Systems in Electric Ships

Airan Frances, *Student Member, IEEE*, Amjad Anvari-Moghaddam, *Senior Member, IEEE*,
 Enrique Rodriguez-Diaz, *Member, IEEE*, Juan C. Vasquez, *Senior Member, IEEE*,
 Josep M. Guerrero, *Fellow, IEEE*, and Javier Uceda, *Fellow, IEEE*,

Abstract—Maritime applications have found in the integration of the electric power system a way to further improve efficiency and reduce the weight of new electric ships. This movement has led scientists to integrate smart management systems to optimize the overall behavior of the grid. In this context, power electronics play a key role in linking the different elements of the power architecture. Moreover, the transition towards a dc distribution, which has already been established in other applications, is being regarded as a promising alternative to ease the integration of renewable sources, batteries, and the ever increasing number of dc loads. In this paper blackbox models are proposed as a tool to foresee the effect of these complex interactions, overcoming the lack of detailed information about the power converters. Large-signal strategies are proposed in order to consider nonlinearities in the static and dynamic behavior of the converters. An accurate model of the physical layer is essential to allow intelligent systems to take the most out of the system performance. This approach offers the opportunity to study the dynamic response of complex interconnected systems, tune the system-level controllers, design protections or assess the compliance of the system dynamics with the standards. Experimental results are included in order to validate the proposed method.

Index Terms—DC-DC power converters, Interconnected systems, Maritime microgrids, Nonlinear dynamical systems, Power system modeling, System dynamics, System identification.

I. INTRODUCTION

NEXT generation of electric ships are expected to improve the power distribution system so that fuel savings, reduced size and weight, and enhanced reliability can be achieved [1]. Some of the strategies proposed to accomplish these objectives are the implementation of dc systems, the inclusion of renewable sources, especially solar energy, and the complete electrification of ships, merging the propulsion system with the rest of the services in an integrated power system [2]–[4]. In this new scenario, the use of energy storage systems provides opportunities to optimize the power management [5], [6].

Intelligent power management systems are being proposed to optimize the power flow within the grid and the dynamic behavior during transients [7]–[9]. In this complex architecture, a dc power distribution entails interesting advantages in terms of simplicity of the power converters and the whole control

This work was supported by the Spanish Ministry of Economy and Competitiveness under the project IDENMRED with reference DPI2016-78644-P and the Consejo social of the Universidad Politécnica de Madrid.

A. Frances and J. Uceda are with the Centro de electrónica industrial, Universidad Politécnica de Madrid, Spain (Tel: +34 91 0676953; e-mail: airan.frances@upm.es; http://www.cei.upm.es).

A. Anvari, E. Rodriguez, J. C. Vasquez, and J. M. Guerrero are with the Department of Energy Technology, Aalborg University, 9220 Aalborg East, Denmark (Tel: +45 2037 8262; Fax: +45 9815 1411; e-mail: joz@et.aau.dk).

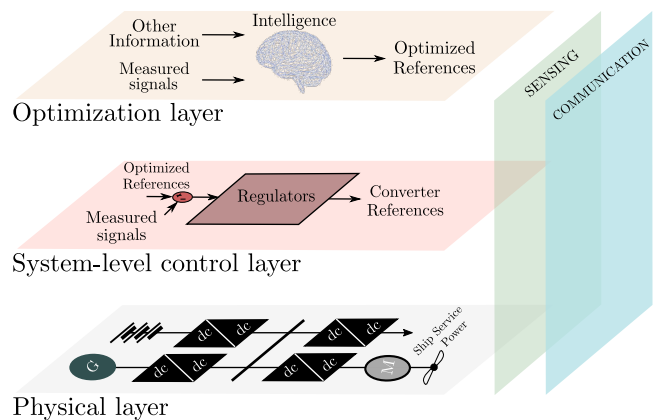


Figure 1: Electric ship intelligent system-level control scheme.

strategy, avoiding extra ac/dc conversions and problems derived by ac distribution as harmonics, synchronization, etc. [10]. Different control strategies proposed for terrestrial dc microgrids can be introduced to maritime applications, as hierarchical control structures [11]. This strategy consists of a primary level, where the voltage or current is regulated; a secondary level, where ancillary services can be included as bus voltage restoration or current sharing; and a tertiary level, where usually power flow is managed by optimization algorithms (Fig. 1).

One of the main differences between terrestrial and maritime dc microgrids is that terrestrial grids generally work in a grid-connected mode, whereas maritime grids work islanded/off-grid in normal operation [12]. Consequently, generation and consumption are of the same order. Furthermore, the length of cables is much shorter in ships. These facts lead to a tightly coupled dynamic behavior and higher effect of transients. Therefore, in this kind of application special attention should be paid to the dynamic assessment of the system, as it has been explicitly recommended in the standards [13], [14]. In this context, obtaining an accurate model of the physical layer is key to design system-level controllers able to follow optimized references, to assess their effect on the interconnected system dynamic, or to study the system stability, which might result in additional restrictions for the optimization algorithms.

The modeling methods used to describe the dynamic behavior of dc power converters can be classified in analytical or blackbox approaches, according to the level of information required; and in linear or nonlinear structures [15]. Analytical approaches are the most popular in the literature [16]–[20], how-

ever in practical applications the use of COTS (Commercial-Off-The-Shelf) converters is advantageous in terms of cost and time to market reduction. Consequently, detailed information about the devices will be limited. Regarding blackbox approaches, the two-port small-signal models are the most extended [21]–[23]. These models are very suitable for dynamic assessment of interconnected systems and stability analyzes, however they are limited to linear systems or applications with a fixed operating point. Blackbox large-signal structures are the most challenging approaches, since they must reproduce nonlinear behaviors of uncertain systems. The need for large-signal approaches in electric ships has been justified in the literature and some analytical solutions can be found in [24], [25]. The literature about blackbox large-signal models able to describe interconnected systems is scarce, the related research works are focused on standalone converters or compared with detailed simulations [26]–[30].

In this paper, a microgrid consisting of generators, storage units, and loads interconnected with a dc bus is considered. These elements are interfaced by means of power converters. In this complex environment, a method to estimate the dynamic behavior of the dc bus is proposed. The approach is based on blackbox large-signal techniques, to deal with the lack of detailed information about COTS converters. The addition of secondary level control layers is also studied, where their effect on the bus dynamic can be checked and the controllers can be tuned if necessary. The results have been validated with laboratory-scaled experiments. The main contributions of this work are summarized as follows:

- Application and experimental validation of the capability of a novel polytopic model with dynamic weighting functions to reproduce the nonlinear behavior of COTS converters.
- A methodology to assess the dynamic performance of secondary controllers applied to COTS converters in a DC integrated power system.
- An interconnection method able to combine the large-signal blackbox models into any desired power distribution structure.

The rest of the paper is organized as follows. The structure of the system considered is presented in Section II. Blackbox modeling techniques are discussed in Section III. The experimental setup used for the validation is introduced in Section IV. The different case studies analyzed are shown in Section V. Finally, the conclusions of the paper are exposed in Section VI.

II. SYSTEM OVERVIEW

The power architecture considered in this work consists of four fundamental elements: generators, storage units, propulsion system, and ship service loads. A scheme of the system is depicted in Fig. 2, where each of these items should have a number of units in parallel, but they have been brought together in order to simplify the diagram. All the elements in the system are interfaced by means of power converters. They contribute by offering controllability of each part of the system and decoupling their dynamics.

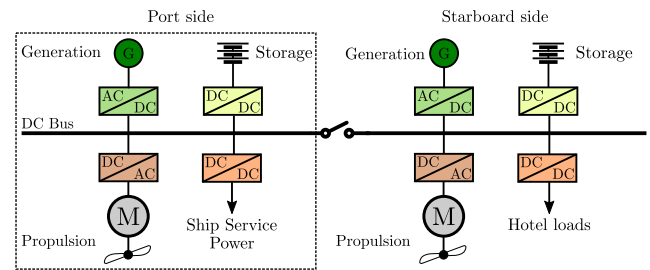


Figure 2: Onboard dc grid scheme.

A hierarchical control structure is considered for the generation and storage units. The primary control is based on droop controllers, to deal with the parallel connection of units regulating the bus voltage. The secondary level includes voltage restoration, which can help to keep the bus voltage within the limits, and current sharing, which could be controlled by algorithms that optimize the power flow among the units. The tertiary level is not considered in this work. However, the extension of the approach to include different buses and their power flows is straightforward, as it will be detailed in the following sections.

The main concern in this power architecture is the dynamic behavior of the dc bus, which is affected by the COTS converters, their control structures and the changes in the load. In this paper the load profile of a drilling vessel with DP (Dynamic Positioning) has been selected as a testbed. The shape of this profile is characterized by different operation modes, which depend on the weather conditions. Four different cases are considered: Mode A for normal DP and normal drilling, Mode B for heavy DP and normal drilling, Mode C for heavy DP and heavy drilling, and Mode D for survival (see Fig. 11). These mission profiles are further detailed in [6].

The next section details the methodology to extract dynamic models from the COTS converters, how to integrate them to the bus architecture in a modular fashion, and how to include system-level controls to these models, in order to predict their effect on the overall dynamic of the system.

III. BLACKBOX MODELING

Blackbox modeling refers to the design of dynamic models of a system whose internal details are unknown. This approach is very useful for power distribution systems based on COTS converter. On the one hand, the manufacturers of the converters will avoid giving detailed information about their devices due to confidentiality issues. On the other hand, it is well-known that the interconnection of power converters can lead to dynamic degraded or even instable systems [31], [32]. These interactions among power converters are especially relevant in maritime applications, where different elements are tightly coupled.

Table I summarizes the different blackbox model structures for dc-dc power converters that can be found in the literature. These structures are classified according to the kind of response they are able to represent. The models are arranged by order of complexity from left to right. The simpler option, the linear model, has been widely used for converters which mostly

Table I: Taxonomy of blackbox models for dc-dc power converters.

| Linear model | Nonlinear model | |
|--|---|--|
| | Static nonlinearity | Dynamic nonlinearity |
| Two-port model: | Wiener-Hammerstein model [26], [27], [33] | Polytopic model [28] |
| •Z-parameters •Y-parameters •H-parameters •G-parameters [21], [23] | | Variation of input variables: Soft Sharp |
| | | Static weighting functions [28] |
| | | Dynamic weighting functions [34] |

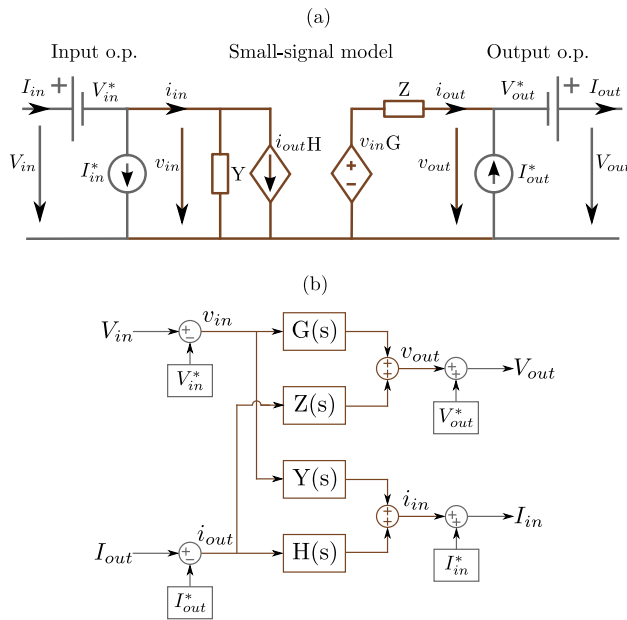


Figure 3: G-parameters model. (a) Equivalent electrical circuit, (b) Block diagram notation.

work in their nominal operating point, taking advantage of the powerful tools available for linear systems to analyze dynamic interactions and stability, as Bode plots and admittance or Nyquist criteria. However, as the power distribution systems become more complex, flexible, and intelligent, the operation conditions of the power converters are more variable, limiting the validity of the small-signal approximations. On the other hand, the nonlinear models can be divided according to the kind of nonlinearity, which can be reflected only in the static behavior of the converter, or also in its dynamic response.

The methodology to obtain the blackbox models is based on the application of perturbations to the system in specific conditions and the identification of transfer functions from its response. In power electronics the most extended structure is the two-port model, where the four variables (input and output currents and voltages) are divided as inputs and outputs of the model. The most popular configuration is to use the input voltage and output current as inputs of the model and output voltage and input current as outputs, which is called G-parameters model (Fig. 3) [22], [35]–[38].

Four transfer functions must be identified to create the model

(1). They are obtained perturbing one of the input variables, while the other input is kept constant, and measuring the response of the output variables. This test will define two of the transfer functions, whereas the reciprocal will define the remaining two. The overall structure constitutes a small-signal model around the operating point in which the variables were kept constant. The perturbation can be performed in frequency or time domain. More details about how to obtain experimentally this kind of model can be found in [21], [23], [39], where techniques to avoid interactions with the source and load used to conduct the tests are proposed.

Audio-susceptibility

$$G(s) = \left. \frac{v_{out}}{v_{in}} \right|_{i_{out}=0}$$

Output impedance

$$Z(s) = - \left. \frac{v_{out}}{i_{out}} \right|_{v_{in}=0}$$

Input admittance

$$Y(s) = \left. \frac{i_{in}}{v_{in}} \right|_{i_{out}=0}$$

Back current gain

$$H(s) = \left. \frac{i_{in}}{i_{out}} \right|_{v_{in}=0}$$

A. System-level control Model

The two-port models described above are able to represent the small-signal behavior of COTS converters. Furthermore, these structures can be modified or combined to form more complex models able to capture nonlinear behaviors, as the ones included in Table I. In this paper the classical two-port network is modified in order to make it possible to integrate a system-level control. The idea is to create a structure that can be used for large-signal analysis and interconnected with other models in any desired architecture.

System-level controllers generally modifies the reference of the controlled variable of the converters [11]. Therefore, by including the transfer functions from the controlled variable to the outputs of the model, it is possible to predict its effect on the dynamic of the converter. The procedure to obtain this new transfer function is analogous to the one presented in the previous Section. A perturbation should be introduced in the reference of the converter, while the other input variables are kept constant in the operating point considered. Particularizing on the G-parameters model of a voltage controlled converter, the following transfer functions can be identified from the response of the output variables to these tests:

$$G_c(s) = \left. \frac{v_{out}}{v_{ref}} \right|_{v_{in}=0, i_{out}=0}$$

$$Y_c(s) = \left. \frac{i_{in}}{v_{ref}} \right|_{v_{in}=0, i_{out}=0}$$

This new input allows the integration of secondary controllers. For instance, to include the effect of a droop control, the reference voltage should be as follows:

$$V_{ref} = V_n - kI_{out}$$

where V_n is the nominal reference value, k is the droop parameter, and I_{out} is the output current of the model.

Similarly, secondary control strategies, as current sharing or voltage restoration, can be implemented by adding the output of

the controllers to the reference value or to the droop parameter. The contribution of this controller, ΔV_{CS} , to the reference voltage (see V_{ref} in Fig. 8) is given by:

$$e = \frac{I_g + I_b}{2} - I_g$$

$$\Delta V_{CS} = \left(K_p + \frac{K_i}{s} \right) e \quad (4)$$

where e is the input of the PI controller, I_g and I_b are the grid and battery currents respectively, and K_p and K_i are the proportional and integral gains of the regulator.

Analogously, the contribution of the voltage restoration controller, ΔV_{VR} , to the reference voltage (see V_{ref} in Fig. 8) is given by:

$$\Delta V_{VR} = \left(K_p + \frac{K_i}{s} \right) (V_{bus} - V_n) \quad (5)$$

where V_{bus} is the bus voltage and V_n is the reference voltage. An example of these implementations is given in the next Section. A PI controller has been used as an example in this work, however any other regulator that affects the reference value of the primary controller of the COTS converter, could be included in the same manner.

B. Large-signal Model

Small-signal models can be very accurate to simulate the response of converters with linear behaviors or applications where the operating point does not differ substantially from the nominal conditions. However, the variability of dc microgrids in general and, specifically, those applied in maritime applications, makes the system work in many different conditions. This fact is particularly relevant in case optimization techniques are applied, which may include nonlinear controllers, different operation modes of the converters or bidirectional power flows.

The nonlinearities in the converters might be reflected fundamentally in their static behavior or they can affect both their static and dynamic behavior. Wiener-Hammerstein models have been proposed to represent the former [27], [33], whereas polytopic models are the ones capable of representing the latter [28], as described in Table I.

The polytopic model is able to represent systems with nonlinear dynamic behavior by integrating small-signal models obtained in different operating points. From a blackbox perspective, the small-signal models are generally two-port models, which are merged in a large-signal model by means of weighting functions, as represented in Fig. 4. In [29], [30], [40] the performance of this technique to analyze dynamic interactions in complex dc distribution systems has been investigated at simulation level. An overview of blackbox modeling techniques can be also found in [15].

In the literature there is a lack of methodologies to optimize the selection of operating points and weighting functions in order to have the maximum accuracy with minimum complexity. A mathematical relationship between the number of operating points and the accuracy of the model, related with the response of the converter, would be of great interest to design efficient models. Besides, polytopic models increase

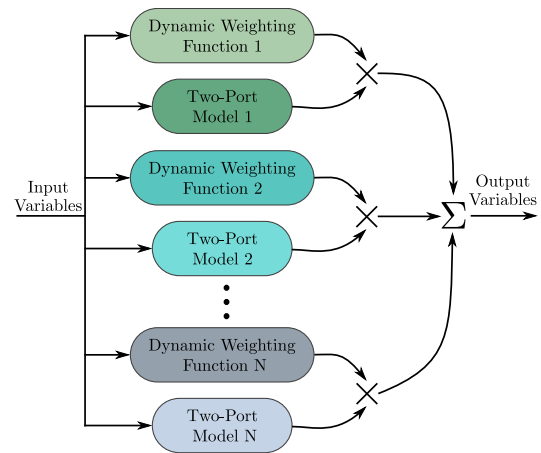


Figure 4: Polytopic model scheme.

their complexity exponentially with the number of operating points considered, so metaheuristic optimization algorithms could be an interesting solution to this problem. In this regard, the development of an automatic procedure to obtain blackbox polytopic models of COTS dc-dc converters is part of the future work.

Double sigmoid is the common choice of weighting function for this kind of model, see (8). Some of the reasons are that they provide flexibility and a smooth result for the transition among small-signal models. However, their suitability for nonlinear systems with sharp variation of the input variables can be compromised. Recently, dynamic weighting functions have been proposed to increase the accuracy of polytopic models in these cases [34].

The weighting functions affect the dynamic behavior of the model. A higher weight is assigned to the small-signal models identified closest to the operating point in which the model is working. The classical weighting functions use the inputs of the model, which in general do not have restrictions in their variation. For instance, in case a given input of the model varies with a step response, the weighting function will change instantaneously the dynamic behavior of the model. However, the rate of change of the system dynamic is limited by its poles, therefore often a certain dynamic in the rate of change of the weighting functions is a better approximation of the real system behavior. In fact, analytical polytopic models commonly use the state variables of the system as inputs of the weighting functions, because they are related with the dynamic of the system by definition. Actually, the dynamic weighting functions are a mean to relate the inputs of the model with the state variables, which can be approximated by means of the poles of the system. The combination of a transfer function, including a selection of the poles of the system, and the static weighting function is called *dynamic weighting function*.

The mathematical justification of this relationship was not included in [34], but it can be derived by representing the state-space equation, applying the laplace transformation and rearranging terms to express the state variables as a function

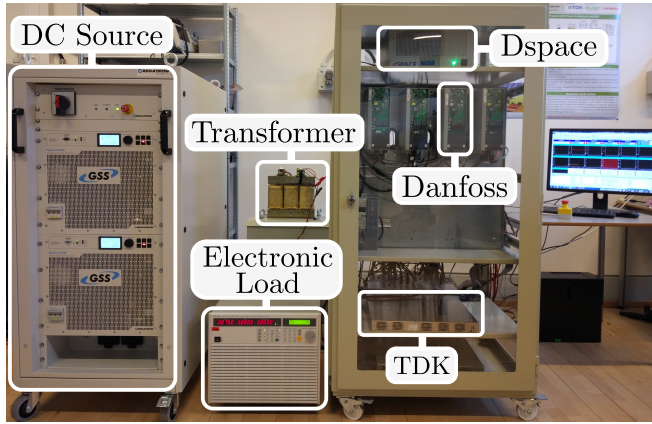


Figure 5: Experimental setup implemented.

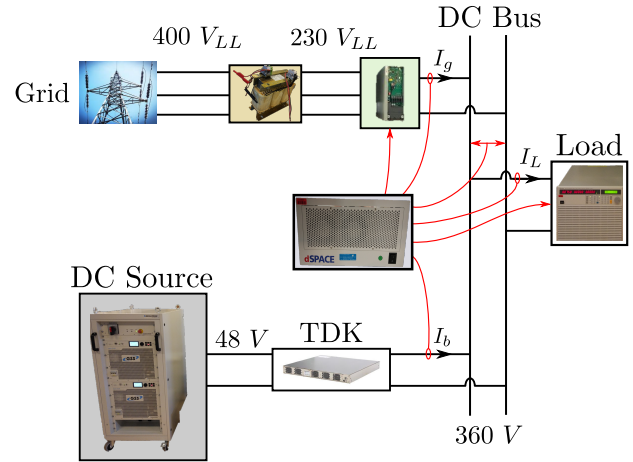


Figure 6: Scheme of the experimental setup.

of the inputs:

$$\begin{aligned}
 \dot{x} &= Ax + Bu \\
 sx &= Ax + Bu \\
 (sI - A)x &= Bu \\
 x &= (sI - A)^{-1}Bu
 \end{aligned} \tag{6}$$

where x is the state vector, u is the input vector, A is the state matrix, B is the input matrix, and I is the identity matrix. This equation clearly shows the relationship between the inputs of a system with their state variables by means of its eigenvalues, which are the poles of the transfer functions identified, in case the states are observable. Therefore, the assumptions made for the use of dynamic weighting functions are validated with this expression. In the next Section this strategy is used to obtain the blackbox model of the rectifier power converter.

IV. EXPERIMENTAL SETUP

A experimental setup (see Fig. 5) has been assembled in order to validate the blackbox modeling techniques described above to predict the dynamic behavior of dc microgrids for maritime applications. In this section it will be described how the system has been arranged and how it has been identified.

A. System Description

The system consists basically of two sources controlling in parallel the bus voltage and an electronic load. It contains the minimum number of elements that allow checking the phenomena of interest, i.e. parallel and series connection of power converters, parallel connection of voltage source converters, secondary-level control strategies and load variations.

One of the sources is a rectifier connected to the electric grid, which will represent the generation units of the ship. A stepdown transformer was introduced to reduce the line to line voltage below the desired bus voltage and to provide galvanic isolation. The bus voltage was set to 360 V in order to keep it safely within the COTS converter rating values. The other source is connected to a 48 V_{dc} power source, which represents a storage unit. These source converters and their blackbox models will be further detailed below. Finally, a Chroma dc electronic load (model 63204) feeds from the dc bus, working

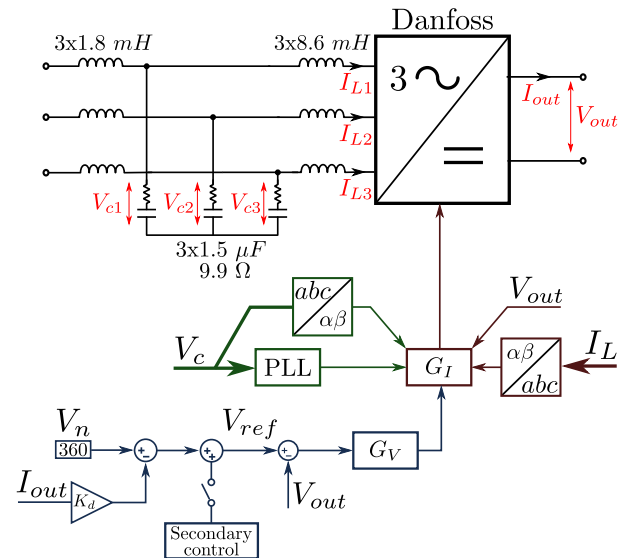


Figure 7: Scheme of the rectifier and its control structure.

as a controlled current load. A hardware-in-the-loop device (Dspace version DS1006) has been used to perform the control of the rectifier, to set the waveform of the current demanded by the electronic load and to capture the currents and voltages of interest. Fig. 6 depicts the scheme of the system described.

B. Rectifier Model

The rectifier converter has been implemented with a Danfoss FC-302 IP20 2.2 kW [41]. This converter has a three-phase IGBT bridge and an EMC filter in the dc side. In the ac side a LCL filter was externally added. The control has been integrated by means of the Dspace HiL device. The control consist of a PLL to synchronize with the grid frequency, an inner input current control and an outer output voltage control to regulate the bus voltage. The inner controller is the one proposed in [42], where a detailed description of the control and its design can be found. The voltage control includes droop control and the possibility to add a secondary control for current sharing or voltage restoration purposes. Fig. 7 depicts the structure described above.

The focus of this work is on the dc part of the rectifier, so no perturbations are considered in the grid voltage. Under this assumption, only the output impedance from the G-parameters (1) is needed to characterize the behavior of the output voltage. Furthermore, the transfer function from the control to the output voltage was identified, in order to be able to account for the effect of secondary controllers.

The output impedance of the rectifier was identified with the grid as a source and the electronic load as the load. The voltage reference was set to 360 V, the droop parameter was set to 0 and no secondary controls were included. The identification was performed in time domain, as the electronic load used is able to provide enough slew rate for the load steps. Notice that in time domain, a high slew rate is necessary to excite high frequencies:

$$slew\ rate \geq 2\pi f A_{pk} \quad (7)$$

where f is the frequency of a sinusoidal signal with a peak value of A_{pk} . The maximum slew rate of the electronic load is $25A/\mu s$. Assuming a $0.5 A_{pk}$ sinusoidal is well above the noise level, the maximum observable frequency is around $8 MHz$, which is much higher than the switching frequency of the converter ($10 KHz$). With this configuration, the electronic load in current mode was set to different current values and steps of 10% of these values were performed to obtain the dynamic behavior of the converter. This value was selected as a good compromise between high enough to avoid the effect of the noise and small enough to ensure a small-signal behavior.

From these tests it was observed that the converter has a different dynamic behavior at light load, I_{out} from 0 to 0.5 A (0-180 W), compared to the behavior at higher values of the load. For values of the output current above 1 A, it was observed that the dynamic behavior did not vary considerably. The data of the response of the output variables to the input perturbations was used in the System Identification toolbox of Matlab in order to obtain the transfer functions. According to the observed behavior of the converter, two transfer functions were obtained: one at $I_{out} = 0.1 A$ and another at $I_{out} = 1 A$. Subsequently, a polytopic model with dynamic weighting functions was designed selecting the poles of the transfer functions that better approximate the transition between small-signal models. Similarly, the G_c transfer functions, described in (2), were obtained at the two operating points mentioned before. Finally, the blackbox model was assembled as sketched in Fig. 8 and the transfer functions obtained are presented in Table II. The static weighting functions used are the classical double sigmoid:

$$\omega_i(I_{out}) = \left(\frac{1}{1 + e^{-m_i(I_{out}-c_i)}} \right) - \left(\frac{1}{1 + e^{-m_{i+1}(I_{out}-c_{i+1})}} \right) \quad (8)$$

where $\omega_i(I_{out})$ are the weighting functions of the small-signal models i , which depend on the output current, I_{out} , m_i and c_i are the slope and the center of the rising edge of the sigmoid and m_{i+1} and c_{i+1} are the slope and the center of the falling edge. In this case, the two models have

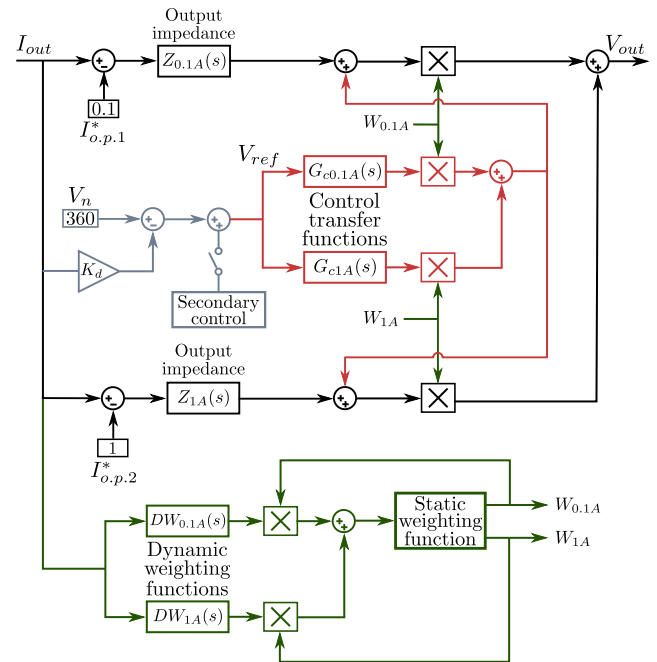


Figure 8: Sketch of the blackbox model of the rectifier.

one interface interval with a slope $m = 20$ and a center in $c = 0.4 A$. These parameters were tuned with the response of the system to a step from one operating point to the other. As mentioned earlier, the identification process of the polytopic models with dynamic weighting functions has been defined in such a way that algorithms can be applied for the automation of the model obtainment. From the response of the system to small and large-signal steps perturbations in the input variables, the program should be able to select the number of operating points to be considered, the slope and center of the weighting functions, and the poles to be included in the transfer functions of the dynamic weighting functions. These decisions are subjected to a trade-of between accuracy and complexity of the overall model.

C. DC-DC Converter Model

The dc-dc converter has been implemented with a TDK-Lambda EZA 2500 2.5 kW bidirectional dc/dc converter 320/48 V (300-380 / 36-60 V) [43]. This converter was used with its own controller and no external components were added. The control includes droop and it can be modified by means of serial communication RS-485. In order to make the identification it was connected to the dc source, a Regatron TopCon TC.GSS, and the electronic load. Once more, the load was set to current mode and 10% steps were performed at different current values. No substantial changes in the dynamic response were observed with the load variation; therefore a small-signal model was enough to represent the converter in the conditions proposed. The integration of the series communication with the HiL program will be considered in future work. In this case, fixed values of the droop parameter were considered. The structure of the blackbox model identified is represented in Fig. 9 and the data is shown in Table II.

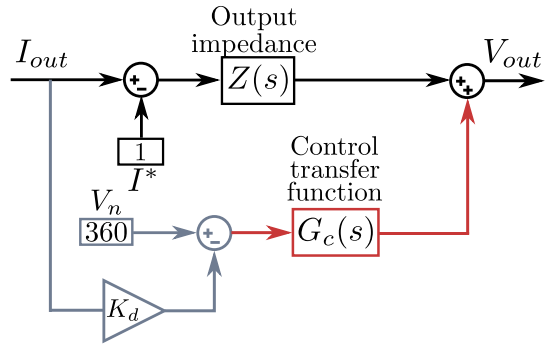


Figure 9: Sketch of the blackbox model of the dc-dc converter.

Table II: Identified data of the blackbox models.

| | |
|--|---|
| $Z_{0.1A}(s) = \frac{932.7s + 3.62e - 10}{s^2 + 10s + 1190}$ | $Z_{1A}(s) = \frac{802s + 6.64e - 10}{s^2 + 20.1s + 1129}$ |
| $G_{c0.1A}(s) = \frac{1507s + 2.05e4}{s^3 + 29.15s^2 + 139s + 2.05e4}$ | $G_{c1A}(s) = \frac{2674s + 5.32e4}{s^3 + 61.7s^2 + 212s + 5.32e4}$ |
| $DW_{0.1A}(s) = \frac{10}{s + 10}$ | $DW_{1A}(s) = \frac{5.14}{s + 5.14}$ |
| $Z(s) = \frac{1402s^2 + 3.03e5 + 2e - 3}{s^3 + 424s^2 + 1.03e5s + 1.01e6}$ | $G_c(s) = \frac{1.8e7}{s^3 + 619s^2 + 1.6e5s + 1.8e7}$ |

In the next section the interconnection of the blackbox described above will be detailed and their performance will be analyzed in different scenarios.

V. CASE STUDIES

An interesting advantage of two-port models is that they can be combined in different ways to create more complex structures. In this section it will be shown how the interconnection of the individual blackbox models can be used to predict the interaction among the converters and their secondary controls. Finally, the simulation results will be validated by comparing them with the real equipment in the same situations.

A. Simulation Results

The previous Sections detailed how to obtain the blackbox models of the different converters used in this work. Now the goal is to use them to be able to simulate the behavior of the system shown in Fig. 6. The idea is to use the outputs of the models as references for controlled sources, which will be connected together to supply the loads. The input of the models, the output current in this case, will be fed back with a current measurement during the simulation. Thus, the only

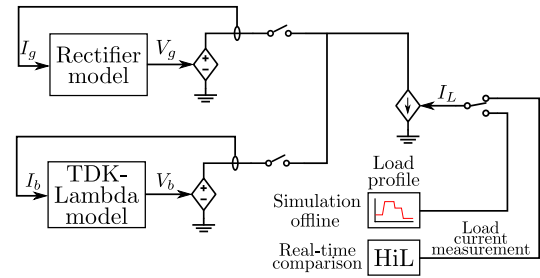


Figure 10: Interconnection of the blackbox models.

input of the model is the current demanded by the load. A sketch of the interconnection of the blackbox models identified is shown in Fig. 10. In this work the focus is on the dc bus, however it would be straightforward to extend this strategy to include the input port of the converters, using current sinks governed by the input current given by the G-parameters model, and measuring the input voltage to feed it back to the model. Those transfer functions have been excluded from this work for purpose of clearness. In addition, the series or parallel connection of further converters is also simple following the same idea.

1) *Interaction Among Converters:* The interconnected model detailed before will be used to study the behavior of the system under different circumstances. In Fig. 11, the dynamic of the signals is compared when only the grid interfacing converter supplies the load and when the battery interfacing converter is connected in parallel. This load profile will be used throughout all the experiments. It represents the different power requirements of a drilling vessel under various conditions as detailed in [6]. The power levels have been scaled to the power ratings of the converters available in the laboratory. The results show how the bus voltage experiences much higher oscillations when only the grid connected converter is supplying the load. At time = 8 s, the second converter is connected and the bus voltage reduces considerably its fluctuation under load steps.

In this example the reference voltage of the battery converter was reduced to 345 V, so it delivers current when the load is high and it stores energy when the load level is low. The droop parameters, k_d were set to 5 and 9.3 for the rectifier and the TDK-Lambda, respectively. From this detailed information about the system dynamics, it would be simple to extract a estimation of the SoC (State of Charge) of the battery, as represented in the results, and the amount of energy that could be extracted during the transients of the system, which are commonly wasted in resistors banks. In this example, if we consider that 1 s corresponds to 1 h, the battery shown would have a capacity of 2.4 kWh. The coulomb county method was used for the SoC estimation, which was considered to start at 50%. The fluctuation of the SoC can be predicted based on the dynamic behavior of the system, which is a valuable information in order to calculate an optimal battery capacity.

2) *Effect of Secondary Control:* The next simulation shows how the behavior of the microgrid is affected when a secondary control is added. In this case, the secondary control shown in Fig. 8 is activated as a current sharing control. A PI controller is added to regulate the output current to be equal to the average

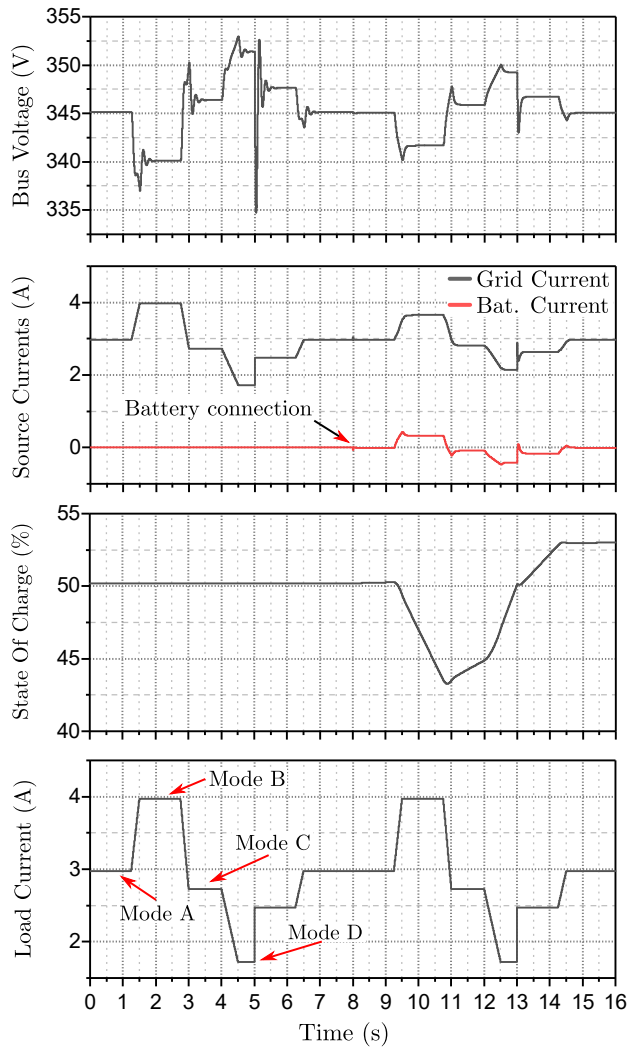


Figure 11: Simulation of how the microgrid dynamic behavior is affected by the parallel connection of the battery and grid interfacing converters.

of both source converters (see (4)). The proportional gain is set to $K_p = 1$ and the integral gain K_i is varied to three different values. In Fig. 12 it is shown that for $K_i = 100$ the transitions are slow and without oscillations. For $K_i = 1000$ the dynamic is faster and some oscillations start to appear and for $K_i = 2000$ the oscillations become considerable. Notice that the model not only shows the expected higher oscillatory behavior when the gain is increased, but also a precise estimation of the actual behavior of the interconnected system, as it will be illustrated in the experimental validation. Therefore, the suitability of this model to design secondary controllers, as well as the possibility of checking the behavior of the converters arranged in different configurations and working in various conditions, is exposed.

B. Experimental Validation

The previous simulations results have been validated comparing the model behavior with the real hardware in similar conditions. In order to perform the comparison, the blackbox model was integrated in the HiL real-time simulator. The load profile was set into the electronic load and the only input

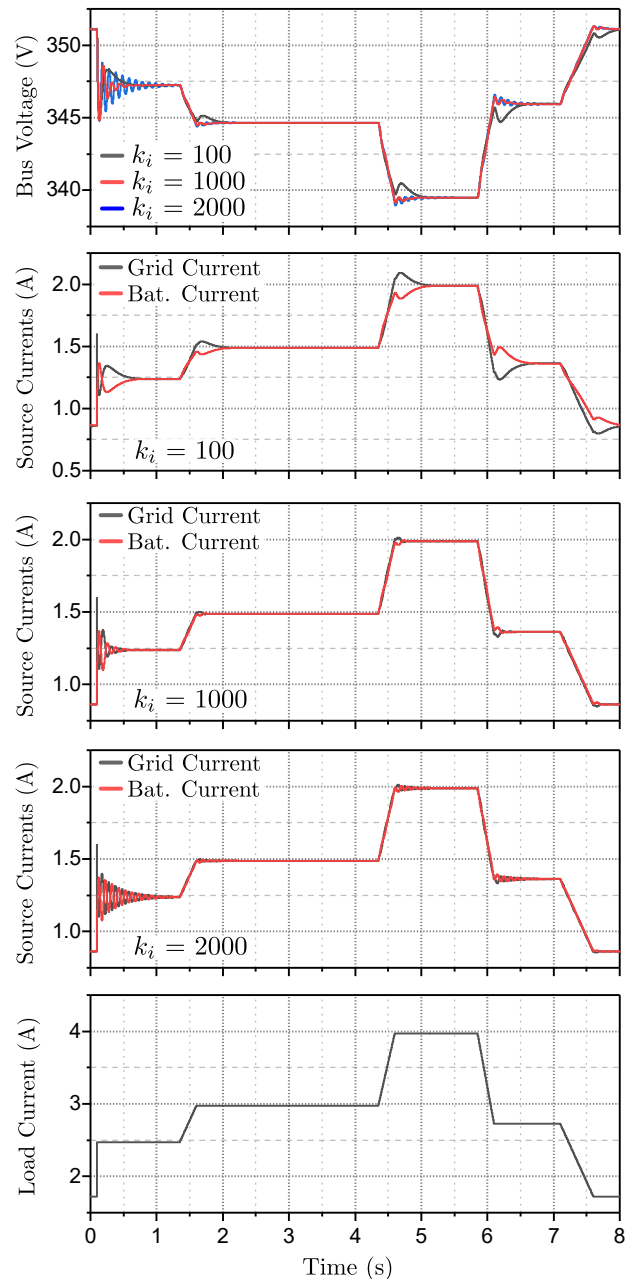


Figure 12: Simulation of how the microgrid dynamic behavior is affected by the design of the current sharing secondary control.

of the blackbox model, I_L from Fig. 10, was included as a measurement of the physical load current. Then the rest of the physical measurements are compared with the model results.

1) *Comparison between small-signal and large-signal models:* The first part of the validation compares the response of the small-signal models and the large-signal model with the setup response. These experiments show that the behavior of the system at low power differs from the behavior at medium and high power.

The first experiment depicts the response of the system when the current sharing control is activated at low power, see Fig. 13. It can be seen that the large-signal model follows the small-signal model identified at low power conditions and it is

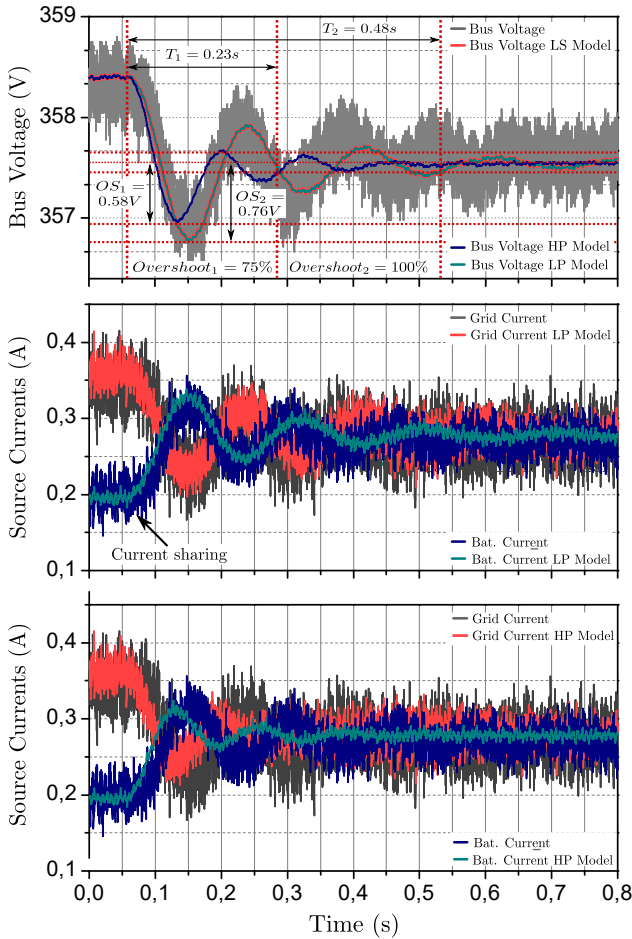


Figure 13: Comparison between the measured signals and the small-signal and the large-signal models response when the current sharing control is activated in low power conditions. LS: large-signal, HP: high power, LP: low power, OS: overshoot

a good estimation of the setup behavior. Compared with the small-signal model identified at high power conditions there is a difference of 25% in the overshoot and twice the settling time of the bus voltage. Also the output currents of the battery and grid interface converters are compared with the small-signal models, but these comparisons are made separately for clarity.

The second experiment is performed in similar conditions but with a higher power demand from the load, see Fig. 14. Again the small-signal and large-signal models are compared with the measured signals from the setup when the current sharing control is activated. In this case, the large-signal model follows the small-signal model identified in high power conditions and it replicates the setup response with a good accuracy. Similarly, the setup behavior differs from the small-signal model obtained in low power conditions in around 25% of overshoot and half the settling time of the bus voltage. As in the previous case, the comparison of the output currents is made separately.

Having shown the suitability of the large-signal model to simulate the system, the next set of experiments will be focused on the capability of the model to include the effect of different system-level controllers and its comparison with the setup

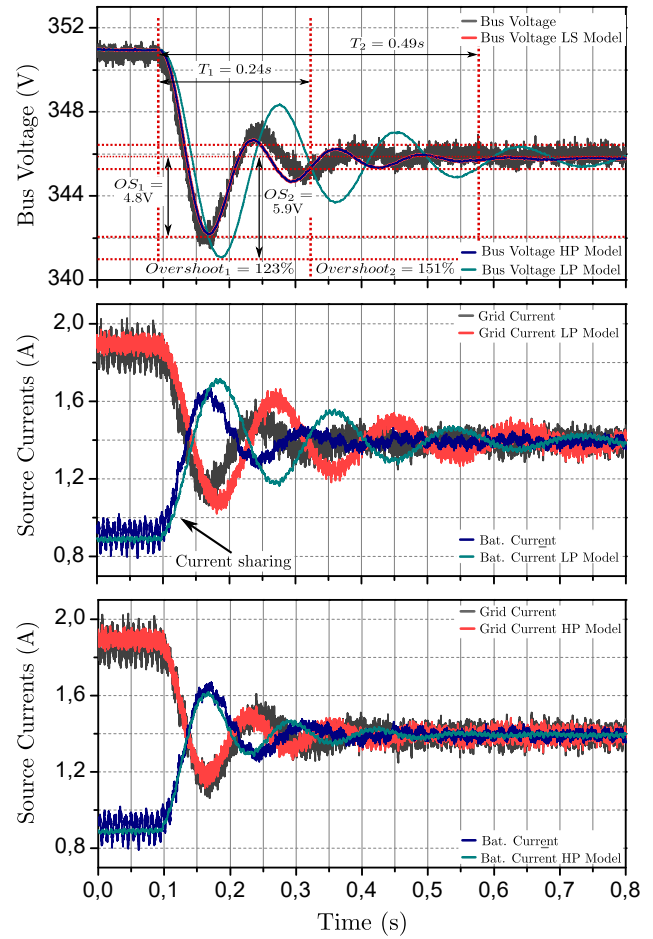


Figure 14: Comparison between the the measured signals and the small-signal and the large-signal models response when the current sharing control is activated in medium power conditions. LS: large-signal, HP: high power, LP: low power, OS: overshoot.

response.

2) *Droop Control*: The first comparison was made without a secondary control. As the dc source was unable to absorb energy, the voltage references of both converters were set to the same value (360 V). The droop parameters, K_d were set to 5 and 9.3 for the grid and battery converters respectively. Fig 15 shows how the model is able to represent precisely the measurements.

3) *Current Sharing*: The next comparison was made adding a current sharing secondary control level (see (4)). The k_i was set to 1000, which was found as a good compromise between fast and low oscillations in the previous simulations. In Fig. 16 the comparison is shown, which includes the activation of the current sharing control loop. The results show how the activation of the current sharing provokes a drop in the bus voltage and it makes the system more oscillatory, as it was expected from the previous simulations. The agreement between model and measurements is very high.

4) *Voltage Restoration*: Finally, a voltage restoration secondary control was added instead of the current sharing control. A PI regulator has been used, comparing the bus voltage with the 360 V reference (see (5)). The proportional gain was

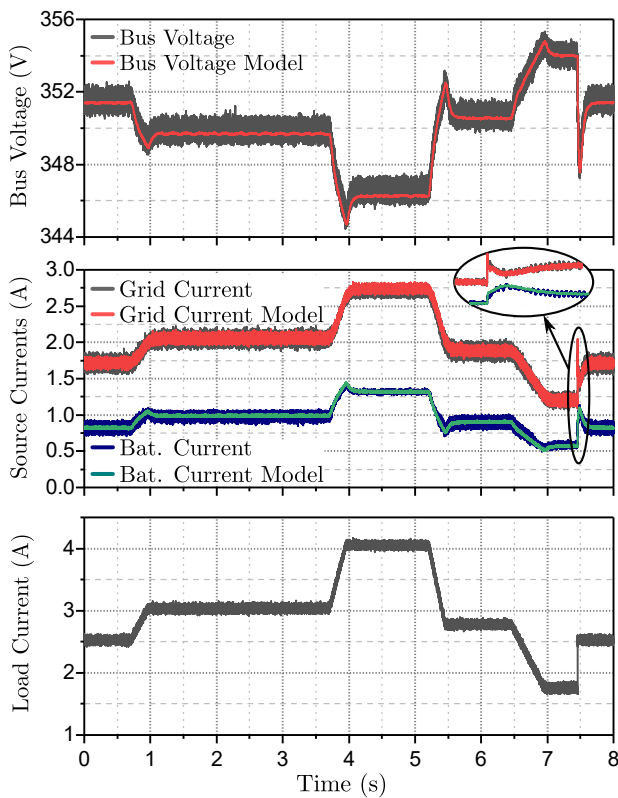


Figure 15: Experimental validation of the blackbox model of the microgrid using droop control.

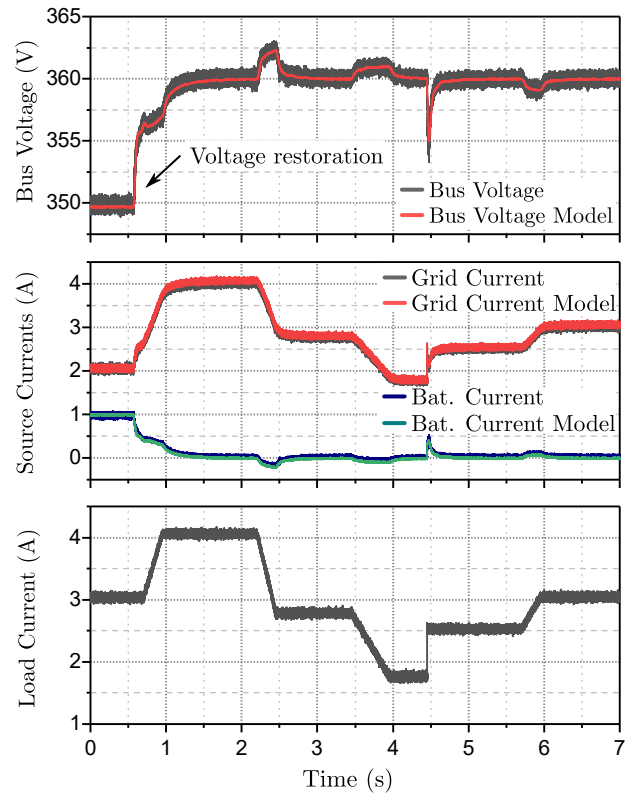


Figure 17: Experimental validation of the blackbox model of the microgrid in the activation of the voltage restoration.

set to 1 and the integral gain was set to 10. In Fig. 17 the activation of the voltage restoration is represented. As this control is only applied to the grid connected converter, most of the load current is supplied by this converter while using this strategy. Once more the model follows the measurements in all conditions. In the future work, the RS485 communication with the TDK converter will be integrated with the Dspace, so both converters can have the secondary control and share the load while performing voltage restoration.

VI. CONCLUSIONS AND FUTURE WORK

The next generation of electric ships is expected to integrate a great deal of power converters. These devices will help to optimize the behavior of the whole system in terms of size, weight, efficiency, reliability, and cost. However, the own nature of the ships, islanded and relatively small compared with terrestrial applications, makes them especially sensitive to dynamic interactions. This issue is particularly relevant when system-level control strategies, nonlinear controllers, or different operation modes are considered. This paper proposes a methodology to study in depth the large-signal interaction of commercial-off-the-shelf power converters in a modular way, so different system configurations can be easily analyzed. Furthermore, a method to predict the behavior of the system when system-level controllers are added to the converters is presented. Finally, the results are validated comparing in real-time the models with the physical system. This methodology can be a useful modeling tool for the system studies advised in the IEEE recommendations for this kind of systems.

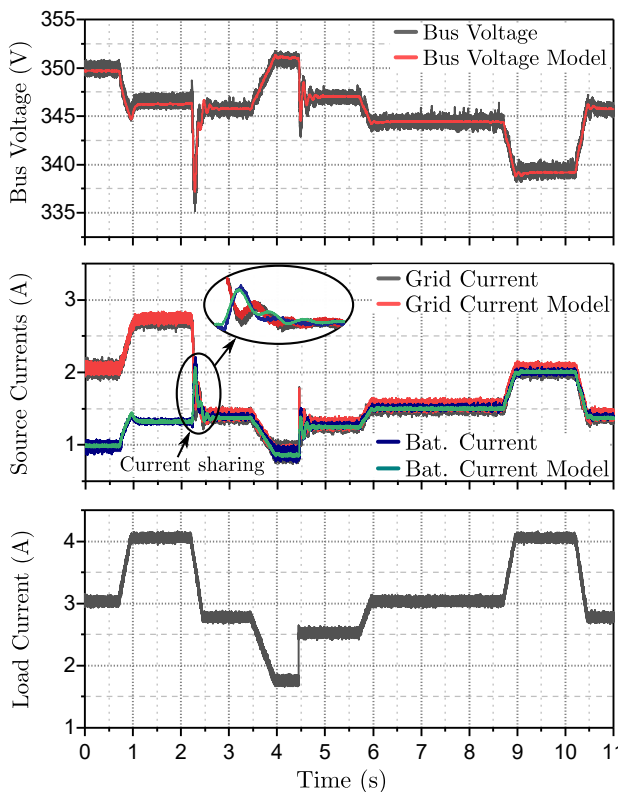


Figure 16: Experimental validation of the blackbox model of the microgrid in the activation of the current sharing.

In the future work the suitability of the proposed methodology will be assessed in different scenarios. Some possibilities are: the use of various kinds of loads, the comparison of the dynamic performance of the bus using different architectures or when several power converters are added with different system-level controllers, converters with different operation modes or nonlinear controllers, etc.

REFERENCES

- [1] S. Mashayekh and K. L. Butler-Purry, "Security constrained power management system for the ng ips ships," in *North Amer. Power Symp.*, Sept 2010, pp. 1–8.
- [2] N. Soltan, H. Stagege, R. W. D. Doncker, and O. Apeldoorn, "Development and demonstration of a medium-voltage high-power dc-dc converter for dc distribution systems," in *Proc. IEEE 5th Int. Symp. Power Electron. Distributed Generation Syst.*, June 2014, pp. 1–8.
- [3] E. Rodriguez-Diaz, F. Chen, J. C. Vasquez, J. M. Guerrero, R. Burgos, and D. Boroyevich, "Voltage-level selection of future two-level lvdc distribution grids: A compromise between grid compatibility, safety, and efficiency," *IEEE Electric. Mag.*, vol. 4, no. 2, pp. 20–28, June 2016.
- [4] F. D. Kanellos, A. Anvari-Moghaddam, and J. M. Guerrero, "A cost-effective and emission-aware power management system for ships with integrated full electric propulsion," *Elect. Power Syst. Research*, vol. 150, pp. 63 – 75, 2017.
- [5] G. J. Tsekouras, F. D. Kanellos, and J. Prousalidis, "Simplified method for the assessment of ship electric power systems operation cost reduction from energy storage and renewable energy sources integration," *IET Electr. Syst. Transp.*, vol. 5, no. 2, pp. 61–69, 2015.
- [6] A. Anvari-Moghaddam, T. Dragicic, L. Meng, B. Sun, and J. M. Guerrero, "Optimal planning and operation management of a ship electrical power system with energy storage system," in *Proc. IEEE Annu. Conf. Ind. Electron. Soc.*, Oct 2016, pp. 2095–2099.
- [7] H. Park, J. Sun, S. Pekarek, P. Stone, D. Opila, R. Meyer, I. Kolmanovsky, and R. DeCarlo, "Real-time model predictive control for shipboard power management using the ipa-sqp approach," *IEEE Trans. Control Syst. Technol.*, vol. 23, no. 6, pp. 2129–2143, Nov 2015.
- [8] L. I. Minchala-Avila, L. Garza-Castanon, Y. Zhang, and H. J. A. Ferrer, "Optimal energy management for stable operation of an islanded microgrid," *IEEE Trans. Ind. Informat.*, vol. 12, no. 4, pp. 1361–1370, Aug 2016.
- [9] F. D. Kanellos, A. Anvari-Moghaddam, and J. M. Guerrero, "Smart shipboard power system operation and management," *Inventions*, vol. 1, no. 4, pp. 1 – 14, 2016.
- [10] S. R. K., P. J. Chauhan, S. K. Panda, G. Wilson, X. Liu, and A. K. Gupta, "An exercise to qualify lvac and lvdc power system architectures for a platform supply vessel," in *IEEE Transp. Electrific. Conf. and Expo, Asia-Pacific*, June 2016, pp. 332–337.
- [11] J. Guerrero, J. Vasquez, and R. Teodorescu, "Hierarchical control of droop-controlled dc and ac microgrids 2014; a general approach towards standardization," in *Proc. IEEE Annu. Conf. Ind. Electron. Soc.*, Nov 2009, pp. 4305–4310.
- [12] Z. Jin, G. Sulligoi, R. Cuzner, L. Meng, J. C. Vasquez, and J. M. Guerrero, "Next-generation shipboard dc power system: Introduction smart grid and dc microgrid technologies into maritime electrical networks," *IEEE Electric. Mag.*, vol. 4, no. 2, pp. 45–57, June 2016.
- [13] *IEEE Recommended Practice for 1 kV to 35 kV Medium-Voltage DC Power Systems on Ships*, Std. IEEE Std 1709-2010, 2010.
- [14] *IEEE Recommended Practice for the Design and Application of Power Electronics in Electrical Power Systems*, Std. IEEE Std 1662-2016 (Revision of IEEE Std 1662-2008), 2017.
- [15] A. Frances, R. Asensi, O. García, R. Prieto, and J. Uceda, "Modeling electronic power converters in smart dc microgrids - an overview," *IEEE Transactions on Smart Grid*, 2017, early access.
- [16] B. Zahedi and L. E. Norum, "Modelling and simulation of hybrid electric ships with dc distribution systems," in *European Conf. Power Electron. Applicat.*, Sept 2013, pp. 1–10.
- [17] M. R. Banaei and R. Alizadeh, "Simulation-based modeling and power management of all-electric ships based on renewable energy generation using model predictive control strategy," *IEEE Intell. Transp. Syst. Mag.*, vol. 8, no. 2, pp. 90–103, Summer 2016.
- [18] J. Kwon, X. Wang, F. Blaabjerg, and C. L. Bak, "Frequency-domain modeling and simulation of dc power electronic systems using harmonic state space method," *IEEE Trans. on Power Electron.*, vol. 32, no. 2, pp. 1044–1055, Feb 2017.
- [19] W. Wu, Y. Chen, A. Luo, L. Zhou, X. Zhou, L. Yang, Y. Dong, and J. M. Guerrero, "A virtual inertia control strategy for dc microgrids analogized with virtual synchronous machines," *IEEE Trans. Ind. Electron.*, vol. 64, no. 7, pp. 6005–6016, July 2017.
- [20] Y. Xu, "Robust finite-time control for autonomous operation of an inverter-based microgrid," *IEEE Trans. Ind. Informat.*, vol. 13, no. 5, pp. 2717–2725, Oct 2017.
- [21] L. Arnedo, D. Boroyevich, R. Burgos, and F. Wang, "Un-terminated frequency response measurements and model order reduction for black-box terminal characterization models," in *Proc. Appl. Power Electron. Conf. Expo.*, Feb 2008, pp. 1054–1060.
- [22] S. Vesti, T. Suntio, J. A. Oliver, R. Prieto, and J. A. Cobos, "Impedance-based stability and transient-performance assessment applying maximum peak criteria," *IEEE Trans. Power Electron.*, vol. 28, no. 5, pp. 2099–2104, May 2013.
- [23] I. Cvetkovic, D. Boroyevich, P. Mattavelli, F. C. Lee, and D. Dong, "Un-terminated small-signal behavioral model of dc-dc converters," *IEEE Trans. Power Electron.*, vol. 28, no. 4, pp. 1870–1879, April 2013.
- [24] B. P. Loop, S. D. Sudhoff, S. H. Zak, and E. L. Zivi, "Estimating regions of asymptotic stability of power electronics systems using genetic algorithms," *IEEE Trans. Control Syst. Technol.*, vol. 18, no. 5, pp. 1011–1022, Sept 2010.
- [25] W. W. Weaver, R. D. Robinett, D. G. Wilson, and R. C. Matthews, "Metastability of pulse power loads using the hamiltonian surface shaping method," *IEEE Trans. Energy Convers.*, vol. 32, no. 2, pp. 820–828, June 2017.
- [26] F. Alonge, F. D'Ippolito, F. M. Raimondi, and S. Tumminaro, "Nonlinear modeling of dc/dc converters using the hammerstein's approach," *IEEE Trans. on Power Electron.*, vol. 22, no. 4, pp. 1210–1221, July 2007.
- [27] J. Oliver, R. Prieto, J. Cobos, O. Garcia, and P. Alou, "Hybrid wiener-hammerstein structure for grey-box modeling of dc-dc converters," in *Proc. Appl. Power Electron. Conf. Expo.*, Feb 2009, pp. 280–285.
- [28] L. Arnedo, D. Boroyevich, R. Burgos, and F. Wang, "Polytopic black-box modeling of dc-dc converters," in *Proc. IEEE Annu. Power Electron. Spec. Conf.*, June 2008, pp. 1015–1021.
- [29] A. Francés, R. Asensi, O. García, R. Prieto, and J. Uceda, "A Black-box Modeling Approach for DC Nanogrids," in *Proc. Appl. Power Electron. Conf. Expo.*, 2016, pp. 1624–1631.
- [30] —, "The performance of polytopic models in smart dc microgrids," in *Proc. IEEE Energy Conversion Congr. Exposition*, Sept 2016, pp. 1–8.
- [31] S. Vesti, T. Suntio, J. . Oliver, R. Prieto, and J. A. Cobos, "Effect of control method on impedance-based interactions in a buck converter," *IEEE Trans. on Power Electron.*, vol. 28, no. 11, pp. 5311–5322, Nov 2013.
- [32] A. Riccobono and E. Santi, "Comprehensive review of stability criteria for dc power distribution systems," *IEEE Trans. Ind. Appl.*, vol. 50, no. 5, pp. 3525–3535, Sept 2014.
- [33] I. Cvetkovic, D. Boroyevich, P. Mattavelli, F. Lee, and D. Dong, "Non-linear, hybrid terminal behavioral modeling of a dc-based nanogrid system," in *Proc. Appl. Power Electron. Conf. Expo.*, March 2011, pp. 1251–1258.
- [34] A. Francés, R. Asensi, O. García, R. Prieto, and J. Uceda, "How to model a dc microgrid: Towards an automated solution," in *Proc. IEEE Second Int. Conf. DC Microgrids*, June 2017, pp. 609–616.
- [35] T. Suntio, M. Hankaniemi, and M. Karppanen, "Analysing the dynamics of regulated converters," *IET IEE Proc. Electric Power Applicat.*, vol. 153, no. 6, pp. 905–910, November 2006.
- [36] M. Hankaniemi, M. Karppanen, T. Suntio, A. Altowati, and K. Zenger, "Source-reflected load interactions in a regulated converter," in *Proc. IEEE Annu. Conf. Ind. Electron. Soc.*, Nov 2006, pp. 2893–2898.
- [37] M. Veerachary and A. R. Saxena, "G-parameter based stability analysis of dc-dc power electronic system," in *Proc. IEEE Joint Int. Conf. Power Syst. Technology Power India Conf.*, Oct 2008, pp. 1–4.
- [38] J. Leppäaho, J. Huusari, L. Nousiainen, and T. Suntio, "Dynamics of current-fed converters and stability-assessment of solar-generator interfacing," in *Proc. IEEE Int. Power Electron. Conf.*, June 2010, pp. 703–709.
- [39] V. Valdivia, A. Barrado, A. Roldan, C. Fernandez, and P. Zumel, "Black-box modeling of dc-dc converters based on transient response analysis and parametric identification methods," in *Proc. Appl. Power Electron. Conf. Expo.*, Feb 2010, pp. 1131–1138.
- [40] A. Francés, R. Asensi, O. García, and J. Uceda, "A blackbox large signal lyapunov-based stability analysis method for power converter-based systems," in *Proc. IEEE Workshop Control Modeling Power Electron.*, June 2016, pp. 1–6.

- [41] Danfoss. (2017) Design guide - vlt automationdrive fc 301/302. Accessed 29 Aug. 2017. [Online]. Available: <http://files.danfoss.com/documents/PE/MG33BF22.pdf>
- [42] F. D. Freijedo, E. Rodriguez-Diaz, M. S. Golsorkhi, J. C. Vasquez, and J. M. Guerrero, "A root-locus design methodology derived from the impedance/admittance stability formulation and its application for lcl grid-connected converters in wind turbines," *IEEE Trans. on Power Electron.*, vol. 32, no. 10, pp. 8218–8228, Oct 2017.
- [43] TDK-Lambda. (2017) Eza datasheet. Accessed 29 Aug. 2017. [Online]. Available: <https://uk.tdk-lambda.com/KB/EZA-Datasheet.pdf>



Airán Francés (S'16) received the M.Sc. degree in electrical engineering from the Universidad Politécnica de Madrid (UPM), Spain, in 2012, where he is currently working toward the Ph.D. degree.

He participated for two years in the European project XFEL, where he collaborated in the design and development of dc/dc power supplies for superconducting magnets. His current research interests include modeling, control and stability assessment of electronic power distribution systems and smart grids.



Amjad Anvari-Moghaddam (S'10, M'14, SM'17) received the Ph.D. degree (Hon.) from University of Tehran, Tehran, Iran, in 2015 in Power System Engineering. Currently, he is a Postdoctoral Fellow and responsible for the IOT MICROGRID LIVING LABORATORY at the Department of Energy Technology, Aalborg University. His research interests include optimal control and management of microgrids. Dr. Anvari-Moghaddam is the Guest Editor of the IEEE TRANSACTIONS ON INDUSTRIAL INFORMATICS special issue: "Next Generation Intelligent Maritime Grids", the journal of APPLIED SCIENCES special issue: "Advances in Integrated Energy Systems Design, Control and Optimization", and the Journal of FUTURE GENERATION COMPUTER SYSTEMS special issue: "Smart Data for Internet of Things". He is also a Technical Committee Member (TCM) of IEEE IES Renewable Energy Systems; TCM-IES Resilience and Security for Industrial Applications (ReSia); TCM-IEEE Working Group P2004 (HIL Simulation and Testing) and Technical Program Committee of iThings-2017, ICIIT-2017, SGIoT-2018, and SmartCity-2018.



Enrique Rodríguez-Díaz (S'15 M'18) received the B.S. degree in electronics engineering and the M.S. degree in sustainable transportation and electrical power systems from the University of Oviedo, Oviedo, Spain, in 2012 and 2014, respectively, and the PhD degree in power electronics from Aalborg Universitet, Denmark, in 2018. His research interests include DC distribution systems, control of power converter units, and microgrids. He is a member of the International Electrotechnical Commission System Evaluation Group SEG4 on Low Voltage DC

Applications, Distribution, and Safety for Use in Developed and Developing Economies. Since 2018 he is Postdoctoral Researcher with the Department of Energy Technology, Aalborg Universitet.



Juan C. Vasquez (M'12, SM'14) received the B.S. degree in electronics engineering from UAM Manizales, Colombia, and the Ph.D. degree in automatic control, robotics, and computer vision from the Technical University of Catalonia, Barcelona, Spain, in 2004 and 2009, respectively. In 2011, He was Assistant Professor and from 2014 He is working as an Associate Professor at the Department of Energy Technology, Aalborg University, Denmark where he is the Vice Programme Leader of the Microgrids Research Program. His current research interests include

operation, advanced hierarchical and cooperative control and the integration of Internet of Things into the SmartGrid. Dr Vasquez is an Associate Editor of IET Power Electronics and in 2017 he was awarded by Thomson Reuters as Highly Cited Researcher. Dr. Vasquez is currently a member of the IECSEG4 on LVDC Safety for use in Developed and Developing Economies, the TC-RES in IEEE Industrial Electronics, PELS, IAS, and PES Societies.



Josep M. Guerrero (S'01, M'04, SM'08, FM'15) received the B.S. degree in telecommunications engineering, the M.S. degree in electronics engineering, and the Ph.D. degree in power electronics from the Technical University of Catalonia, Barcelona, in 1997, 2000 and 2003, respectively. Since 2011, he has been a Full Professor with the Department of Energy Technology, Aalborg University, Denmark, where he is responsible for the Microgrid Research Program (www.microgrids.et.aau.dk). From 2012 he is a guest Professor at the Chinese Academy of

Science and the Nanjing University of Aeronautics and Astronautics; from 2014 he is chair Professor in Shandong University; from 2015 he is a distinguished guest Professor in Hunan University; and from 2016 he is a visiting professor fellow at Aston University, UK, and a guest Professor at the Nanjing University of Posts and Telecommunications. His research interests are oriented to different microgrid aspects, including power electronics, distributed energy-storage systems, hierarchical and cooperative control, energy management systems, smart metering and the internet of things for AC/DC microgrid clusters and islanded minigrids; recently specially focused on maritime microgrids for electrical ships, vessels, ferries and seaports. Prof. Guerrero is an Editor for several journals. He was the chair of the Renewable Energy Systems Technical Committee of the IEEE Industrial Electronics Society. He received the best paper award of the IEEE Transactions on Energy Conversion for the period 2014-2015, and the best paper prize of IEEE-PES in 2015. As well, he received the best paper award of the Journal of Power Electronics in 2016. In 2014, 2015, and 2016 he was awarded by Thomson Reuters as Highly Cited Researcher, and in 2015 he was elevated as IEEE Fellow for his contributions on "distributed power systems and microgrids."



Javier Uceda (M'83, SM'91, F'05) obtained the M.Sc. and Ph.D. degrees in Electrical Engineering by the Universidad Politécnica de Madrid (UPM), Spain in 1976 and 1979 respectively.

He is currently Full Professor in Electronics in the Electrical and Electronic Engineering Department at UPM. His research activity has been developed in the field of Power Electronics where he has participated in numerous national and international research projects. His main contributions are in the field of switched-mode power supplies and dc/dc power converters for telecom and aerospace applications. As a result of this activity he has published more than two hundred and fifty papers in international journals and conferences and he holds several national and international patents.

Prof. Uceda has received several individual and collective awards like the IEEE Third Millennium Medal, the Puig Adán Medal. He is also Honorary Doctor by the Universidad Ricardo Palma in Perú and the Colegio de Posgraduados in Mexico.